JOURNAL OF SPACECRAFT AND ROCKETS
Vol. 38, No. 5, September–October 2001

Low-Cost Main-Belt Asteroid Sample Return

Alexander A. Sukhanov*
Russian Academy of Sciences, GSP-7.117997, Moscow, Russia
Otávio Durão†
National Space Research Institute, 12210-40 São José dos Campos, Brazil
and
Daniela Lazzaro‡
National Observatory, 20921-400 Rio de Janeiro, Brazil

A main-belt asteroid sample return without landing on the asteroid is proposed. The spacecraft collects the sample during the asteroid flyby, crossing the dust cloud produced by a projectile, and delivers the sample to the Earth. To lower the launch energy, the spacecraft uses a Venus and Earth gravity assist trajectory type maneuver. Five launch windows in the 2004–2010 period are considered, offering several mission options, with the respective results of the trajectory design. Most mission options offer other asteroid encounters in addition to the primary target. On completion of the primary sample return mission, the spacecraft can swing by the Earth to fly by additional asteroids or a comet. Secondary targets and possible mission extensions are considered for some of the mission options. Spacecraft navigation and the projectile targeting are also discussed, as well as estimates of the mass of the sample to be collected. The sample ejection considers two projectile types: passive, using only the impact energy, and active, carrying an explosive inside.

Nomenclature

C_3	=	launch energy, km^2/s^2
D	=	projectile miss of the nominal impact point in B-plane, km
E	=	impact energy, MJ
h	=	distance between the projectile impact point and the spacecraft path (see Fig. 4), km
L_1	=	2004 launch window (17 February 2004–12 May 2004)
L_2	=	2005 launch window (18 September 2005–9 December 2005)
L_3	=	2007 launch window (1 April 2007–25 July 2007)
L_4	=	2008–2009 launch window (17 November 2008–7 March 2009)
L_5	=	2010 launch window (5 June 2010–13 October 2010)
M	=	ejected mass, kg
m	=	projectile mass, kg
m_e	=	explosive mass, kg
R	=	maximum particle distance from the impact at time $\tau(R = U\tau)$, km
r	=	distance from the impact point to the spacecraft, km
S	=	area of the sample collector, m^2
t_s	=	time between the projectile separation and the closest approach, s
U	=	maximum ejection velocity, km/s
u	=	ejection velocity, km/s
V	=	ejecta volume, km^3
v	=	spacecraft flyby velocity, km/s
x	=	spacecraft position in the flyby trajectory measured from closest approach to impact, km
ΔV	=	velocity increment for orbital maneuver, km/s
Δv	=	projectile separation velocity, m/s
Δv_t, Δv_n	=	tangent and normal components of the separation velocity, m/s
δd	=	uncertainty in the asteroid flyby distance, determined before the projectile separation, km
δh	=	uncertainty in the distance h stipulated by $\delta\sigma$, km
$\delta\sigma$	=	projectile angular separation error, deg
η	=	impact or explosive effectiveness
λ	=	constant, kg · s/km
μ	=	collected sample mass, mg
ρ	=	spatial density of the dust cloud, kg/km^3
σ	=	projectile separation angle, arctan$(\Delta v_n/\Delta v_t)$, deg
τ	=	time between impact and spacecraft closest approach to impact point, s
$\varphi_1, \varphi_2, \psi$	=	angles for sample ejection model defined in Figs. 5 and 6, deg
χ	=	specific energy of the explosive, MJ/kg

Received 3 March 2000; revision received 12 April 2001; accepted for publication 11 May 2001.

*Senior Researcher, Flight Dynamics and Data Processing Division, Space Research Institute; currently Visiting Researcher, Space Mechanics and Control Division, National Space Research Institute, 12210-40 São José dos Campos, Brazil.
†Senior Engineer, Space Mechanics and Control Division.
‡Senior Researcher, Astrophysics Department.

Introduction

THE main-belt asteroid sample return is of great interest for science because it can answer many questions about the solar system origin. However the conventional way for the sample return, including landing on the asteroid, is quite costly because the main-belt asteroid flyby velocity is higher than 4 km/s. This flyby velocity requirement means that a ΔV greater than 8 km/s is needed to land the spacecraft on the asteroid and then to launch it back to the Earth. According to a very optimistic assessment, to return a 200-kg spacecraft with recoverable capsule containing the sample to the Earth, the initial three-stage spacecraft mass should be about 7 metric tons. The problem could be solved using solar electric propulsion (SEP). However, use of SEP generates other problems, such as the necessity of large solar panels and the difficulty of control.

NASA Stardust comet sample return mission uses an alternative method for the sample return, which does not include landing. This alternative sample collection procedure was also independently considered for the proposed phobos sample return mission[1] and the proposed Aladdin Phobos and Deimos sample return mission. The alternative mission concept is the following: 1) The spacecraft is launched into a trajectory that performs a rendezvous with the asteroid and returns to the Earth. 2) Before the encounter, a projectile is separated from the spacecraft, which hits the asteroid and produces a dust cloud. 3) The spacecraft crosses the cloud and picks up the dust particles into a collector. 4) The collected samples are placed into a recoverable capsule, which is detached from the spacecraft before reentry into the Earth's atmosphere. In the present paper some asteroids of different existing classes were selected as possible

targets of a sample-return mission, based on the scientific return that its analysis will bring to a more complete understanding of the formation and evolution of the asteroids and the solar system as a whole.

This approach will be further detailed in the remainder of this work, considering asteroids located in the main belt. It is also proposed to use a Venus and Earth gravity assist (VEGA) maneuver for the spacecraft launch to the main belt. The VEGA maneuver significantly lowers the launch energy. Thus, the considered mission concept performs the sample return with low launch energy and without any significant midcourse maneuver. A very close approach to the asteroid will be needed, but the Deep Space 1 (DS1) mission has proven that this is possible.[2,3] Note that a few more asteroids can be also encountered as secondary targets during the extended mission.

Selection of Mission Targets

To understand correctly the formation and evolution of our solar system, it is important to analyze some of its most primitive objects, such as asteroids and comets. The mineralogical composition of the asteroids can indicate not only the elements present in the solar nebula, but especially the thermal processes undergone by these objects since their formation. Note that the present mineralogical composition and structure of an asteroid is a direct consequence of the degree of heating it has passed through. In this sense, the most primitive objects would be those that have undergone no thermal processes, preserving an original homogeneous composition.

The surface mineralogical composition of asteroids can be inferred through diverse techniques[4] such as photometry and spectroscopy in the visible and near-infrared region. The diverse data set with information about the surface characterization of a great number of asteroids permits the organization of them in classes.[5] Disregarding small details, most of the taxonomies define an S class (metal plus olivine plus pyroxene), recently divided in seven subclasses from S(I) up to S(VII); a C class (carbon plus hydrated silicates plus organic material); a D and/or P class (anhydrited silicates plus carbon plus organic material), an M and/or E class (metal plus enstatite); and a V class (pyroxene plus feldspar).

The basic question is to understand the degree of differentiation undergone by the distinct classes of asteroids. In a differentiation process, the object undergoes a complete melting with subsequent separation of the materials, based on their density. If a collision would disrupt such a body the fragments from the core would be classified as M, those from the mantle as S(I) or E, and those from the crust as S(VI), S(VII), or V. This model, although very simple and compatible with laboratory experiments, has been questioned due to the high temperatures needed to differentiate bodies of the size of asteroids in the early phases of the solar system formation. On the other hand, the asteroid 4 Vesta has been known as the only big asteroid that apparently has undergone a complete differentiation process. The comparison in laboratory of lunar samples with those from Vesta will help to solve the fundamental question about this asteroid: Why is it the only one that produced a basaltic crust? The same question can be answered by the analysis of a sample from 2 Pallas, which is larger than 4 Vesta. Therefore, some asteroids of each class were selected as possible targets of a sample-return mission, based on the scientific return that its analysis will bring to a more complete understanding of the formation and evolution of the asteroids and the solar system as a whole.

Mission Opportunities

We consider spacecraft trajectories to the main belt of asteroids and returning to the Earth in two or three years. The direct flight requires a launch energy C_3 of 37.7 and 83.4 km^2/s^2 for the two- and three-year flights, respectively. The VEGA maneuver can provide both two- and three-year Earth–asteroid–Earth loops with C_3 from 9 to 15 km^2/s^2. Therefore, the direct flight to the main belt is not considered in this paper despite that the VEGA maneuver makes the mission longer by 12–17 months. Thus, the total mission duration in the case of the VEGA maneuver is between 3 and 4.45 years. The maneuver also limits the number of the reachable asteroids, although this number is still quite considerable. It is also possible

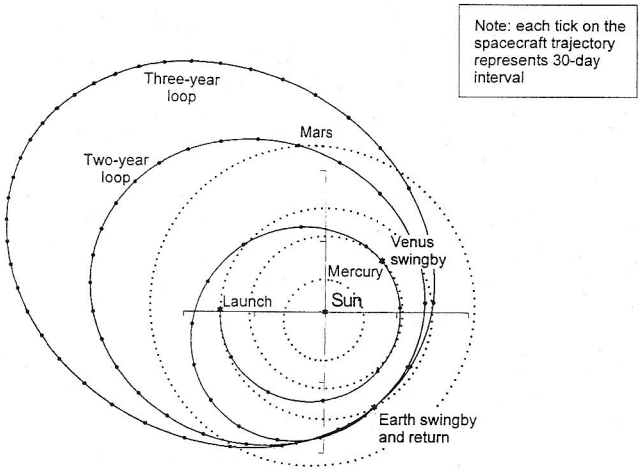

Fig. 1 Spacecraft trajectory returning to Earth two and three years after the VEGA maneuver.

to insert the spacecraft into a heliocentric orbit of 2.5-year period after the VEGA maneuver with return to the Earth in five years after the Earth swingby, that is, after two revolutions of the spacecraft and five revolutions of the Earth around the sun. The paper does not consider such a mission because the duration is too long.

Note that the return to the Earth in two years after the Earth swingby makes the mission shorter (three-year mission), but in this case the spacecraft reaches just a narrow internal part of the main belt, whereas in the case of the return in three years after the swingby (four-year mission), the spacecraft trajectory covers the entire belt. Figure 1 shows the belt coverage. Also, contrary to the four-year mission, it is nearly impossible to encounter more asteroids (secondary targets) for a reasonable additional ΔV in the three-year mission. However, this disadvantage can be compensated by an extended mission. A subsequent section of the paper gives more details about the secondary targets and mission extensions.

Spacecraft launch is within the time frame 2004–2010. There are five launch windows L_{1-5} within that period when the VEGA maneuver can be performed with launch energy $C_3 \leq 15$ km^2/s^2. The launch windows are defined in the Nomenclature section. The selection of the asteroids for the mission used the following constraints: 1) taxonomic types V, M, E, P, D, S(I), S(IV), S(VII), and B-type asteroid 2 Pallas; 2) asteroid diameters ≥ 20 km; 3) launch energy $C_3 \leq 15$ km^2/s^2; and 4) midcourse $\Delta V \leq 0.5$ km/s.

Table 1 shows the asteroids that can be taken as candidates for the sample-return mission under the given constraints. Note that there are many other asteroids of the selected taxonomic types that can be encountered for the considered launch dates (especially asteroids of the numerous M and S types). Nevertheless, Table 1 indicates a significant number for the mission targets for the subsequent analysis. Table 1 also shows the asteroid spin rates and their reliability.[6]

The mission options are considered in more detail. The trajectory design for the options uses the patched-conic approach. The planet state vectors were derived from the compressed ephemeris using the SOLSYS FORTRAN routine, both developed by the U.S. Naval Observatory in 1987–1988. The asteroid states were taken from the Bowell's orbital elements[7] and then propagated using the Runge–Kutta-8 propagator taking into account perturbations of all of the planets. Table 2 gives the following parameters for a 10-day launch periods: launch and asteroid flyby dates, total mission duration, launch energy C_3, total necessary midcourse ΔV, asteroid flyby velocity, reentry velocity into the Earth atmosphere, distances from the sun and Earth during the asteroid encounter, sun–Earth–spacecraft (S–E–SC) angle during the encounter, and the asteroid illumination phase, that is, the illuminated fraction of the asteroid front view as seen from the approaching spacecraft.

Launch in 2004

Table 2 shows that there are three mission options for 113 Amalthea asteroid: two three-year missions, which differ by the date of the asteroid encounter, and one four-year mission option.

Table 1 Primary targets

Asteroid	Diameter, km	Taxonomy type	Spin rate, h	Reliability[a]	Launch window
2 Pallas	525.0	B	7.813	a	L_3
4 Vesta	510.0	V	5.342	a	L_2
7 Iris	203.0	S(IV)	7.139	a	L_5
8 Flora	141.0	S(IV)	12.8	c	L_3, L_4
16 Psyche	264.0	M	4.196	a	L_1
21 Lutetia	99.5	M	8.16	b	L_2, L_3, L_4
27 Euterpe	131.0	S(IV)	11	d	L_2, L_3, L_5
33 Polyhymnia	65.8[b]	S(IV)	18.60	b	L_5
40 Harmonia	111.0	S(VII)	8.9	c	L_4
44 Nysa	73.3	E	6.421	a	L_5
55 Pandora	67.5	M	4.804	a	L_1, L_5
56 Melete	117.0	P	18.14	b	L_2
64 Angelina	63.1[c]	E	8.755	a	L_2, L_3
67 Asia	60.3	S(IV)	15.9	c	L_1, L_2
69 Hesperia	143.0	M	5.66	b	L_3
75 Eurydike	58.3	M	5.36	b	L_4
80 Sappho	81.7	S(IV)	14.03	b	L_4
102 Miriam	86.0	P	——	——	L_3
110 Lydia	89.1	M	10.92	b	L_3
113 Amalthea	47.6	S(I)	9.9	c	L_1, L_3
115 Thyra	83.5	S(IV)	7.2	c	L_4
140 Siwa	114.0	P	——	——	L_5
161 Athor	45.7	M	7.29	b	L_5
214 Aschera	26.8	E	6.8	c	L_2
250 Bettina	85.5	M	5.054	a	L_2
317 Roxane	22.6	E	8.17	b	L_1, L_2
336 Lacadiera	72.0	D	13.73	b	L_3, L_5
406 Erna	53.8	P	——	——	L_1, L_4
613 Ginevra	82.0	P	——	——	L_4
773 Irmintraud	99.1	D	——	——	L_1
1036 Ganymed	38.5	S(VII)	10.31	b	L_3

[a]Reliability of the spin rate knowledge: a, reliable pole position exists; b, a very accurate synodic rotation period is available; c, the error in the rotation period is smaller than 1 h; and d, the error is several hours.
[b]Diameter was calculated assuming albedo = 0.16, typical for S-type asteroids.
[c]Diameter was calculated assuming albedo = 0.38, typical for E-type asteroids.

The first three-year option has slightly bigger launch C_3 than the second one. However the first three-year option has an advantage: The phase during its approach is better than in the second three-year option because the spacecraft approaches the asteroid in the ascending part of its trajectory. (The asteroid phase is 0.76 in the first option and 0.22 in the second option; see Table 2.) There are also two options for the asteroid 317 Roxane sample return: three-year and four-year options. The communication conditions during the asteroid encounter are sufficiently favorable for all of the mission options, that is the angle S–E–SC is large enough.

Launch in 2005

This year is the only launch year among the considered ones when a V-type Vesta asteroid sample can be returned. Table 2 shows that the launch in 2005 is characterized by higher (on average) asteroid flyby velocities compared to launch in 2004. The communication conditions are favorable for all of the mission options.

There are two options (three- and four-year mission durations) for Vesta and Lutetia; each of the options has advantages and disadvantages. Advantages of the three-year Vesta mission are its short time frame and low flyby velocity. However, in the four-year mission, the launch C_3 is lower, and the communication conditions during the encounter are better. (The encounter is closer to the Earth.) Note that both 64 Angelina and 214 Aschera asteroids can be encountered in one mission as the next section of the paper shows.

Launch in 2007

Table 2 indicates that the Pallas sample can be returned if the launch is in 2007. Table 2 also shows that midcourse active maneuvers (with ΔV ranging from 30 to 500 m/s) are needed for all options of the 2007 launch year. The asteroid flyby velocities are higher, on the average, than those for launch in 2004. However, there is an option with the lowest flyby velocity among all of the considered options within all launch dates (102 Miriam, 4 km/s; see Table 2). The communication conditions during the encounter are poor for 2 Pallas, 69 Hesperia, and 110 Lydia and just slightly better for 1036 Ganymed because of the very narrow S–E–SC angle.

Launch in 2008–2009

In the case of launching in 2008–2009, the return to the Earth three years after the VEGA maneuver, that is, the four-year missions, needs rather high launch C_3 (406 Erna; see Table 2) or a significant ΔV during the Earth swingby to be performed in 2010 as a part of the VEGA maneuver (21 Lutetia and 613 Ginevra; see Table 2). Thus, as Table 2 shows, the mission duration is 3–3.4 years for most of the options. The communication angles are favorable in all cases except for the 613 Ginevra option.

Launch in 2010

Note that the launch in 2010 allows the lowest launch C_3 (less than 8.4 km^2/s^2) for performing the VEGA maneuver among all considered launch dates. However, as Table 2 shows, all of the options need launch C_3 greater than 10 km^2/s^2. Thus, the lowest launch energy is not actualized in the specific mission options. The asteroid flyby velocities are rather high, and the communication angles are relatively favorable for all of the options. The 44 Nysa and 336 Lacadiera asteroids can be encountered in one mission. This possibility will be considered in more detail in the next section.

Secondary Targets and Mission Extensions

Most of the mission options considered allow close approach to one or more asteroids with a reasonable additional ΔV. This extension of the mission is mainly true for the four-year missions having longer duration and covering the entire main belt. However, in most cases only small unnumbered asteroids are among the secondary targets.

The asteroid sample-return mission can be extended as follows: After the recoverable capsule is detached to reenter the Earth atmosphere, the spacecraft can be targeted to another asteroid or a comet using EGA. There are many asteroids that can be reached during the

Table 2 Mission parameters

Asteroid	Launch period	Date of flyby	Mission duration, yr	Launch C_3, km^2/s^2	Midcourse ΔV, km/s	Flyby velocity, km/s	Reentry velocity, km/s	Distance from sun, AU	Distance from Earth, AU	S–E–SC angle, deg	Phase (1 = full)
16 Psyche	March 2004	17 Jan. 2007	4.33	8.84	0.00	4.53	14.4	3.19	2.49	127	0.43
55 Pandora	March 2004	7 June 2007	4.35	9.42	0.15	6.03	14.5	3.11	3.19	77	0.18
67 Asia	April 2004	27 Dec. 2007	4.33	8.93	0.00	6.84	14.4	2.45	2.93	52	0.10
113 Amalthea	March 2004	13 July 2006	3.31	9.39	0.00	6.11	14.3	2.23	3.05	30	0.76
113 Amalthea	April 2004	8 Dec. 2006	3.34	8.90	0.00	6.50	14.5	2.17	2.85	39	0.22
113 Amalthea	April 2004	15 April 2006	4.37	8.88	0.00	12.40	14.5	2.30	2.30	77	0.96
317 Roxane	March 2004	4 June 2006	3.01	12.68	0.00	5.86	13.7	2.21	3.16	17	0.21
317 Roxane	March 2004	18 Dec. 2007	4.33	9.24	0.06	8.69	14.4	2.44	2.90	53	0.04
406 Erna	March 2004	7 Dec. 2006	4.29	11.34	0.27	4.73	14.5	3.18	2.61	116	0.36
773 Irmintraud	March 2004	16 Oct. 2006	4.34	8.97	0.05	7.56	14.4	3.07	3.65	48	0.77
4 Vesta	Nov. 2005	16 Dec. 2007	3.16	15.00	0.25	5.26	14.4	2.24	2.99	34	0.56
4 Vesta	Oct. 2005	23 Aug. 2007	4.26	10.44	0.22	11.21	14.3	2.16	1.77	99	0.95
21 Lutetia	Oct. 2005	12 Oct. 2007	3.19	14.46	0.05	8.84	14.2	2.11	2.29	67	0.88
21 Lutetia	Oct. 2005	22 Aug. 2007	4.24	10.46	0.43	14.23	14.3	2.18	1.79	98	0.97
27 Euterpe	Nov. 2005	10 Feb. 2008	3.27	11.41	0.00	7.21	14.6	2.25	3.05	31	0.86
56 Melete	Oct. 2005	23 May 2008	3.20	13.62	0.00	10.62	14.2	2.09	2.48	56	0.11
64 Angelina	Nov. 2005	13 March 2008	4.26	10.27	0.03	7.02	14.8	2.99	3.92	18	0.90
67 Asia	Nov. 2005	28 July 2009	4.26	10.58	0.00	14.13	14.5	2.33	2.59	64	0.03
214 Aschera	Nov. 2005	5 June 2009	4.25	10.49	0.34	8.85	14.8	2.61	3.38	35	0.08
250 Bettina	Nov. 2005	13 March 2009	4.27	13.02	0.00	6.94	14.7	2.97	3.83	26	0.30
317 Roxane	Oct. 2005	1 Aug. 2009	4.23	11.26	0.34	12.83	14.4	2.13	1.94	86	0.03
2 Pallas	May 2007	24 Sept. 2009	3.45	8.99	0.05	12.82	13.9	2.28	3.28	6	0.36
21 Lutetia	May 2007	12 Feb. 2011	4.27	10.84	0.23	7.51	14.3	2.38	2.68	62	0.08
27 Euterpe	May 2007	11 May 2009	4.40	14.19	0.21	8.42	14.3	2.19	1.95	89	0.93
64 Angelina	May 2007	10 Dec. 2010	4.24	9.05	0.45	11.10	14.3	2.61	3.39	32	0.05
69 Hesperia	May 2007	9 Oct. 2010	4.25	10.18	0.50	10.64	14.3	2.81	3.81	1	0.07
102 Miriam	June 2007	24 April 2010	4.29	14.24	0.17	4.09	14.4	3.21	2.22	168	0.73
110 Lydia	June 2007	12 Nov. 2010	4.27	11.63	0.23	7.04	14.4	2.81	3.79	4	0.14
113 Amalthea	May 2007	2 April 2011	4.43	14.92	0.34	12.54	14.6	2.30	2.39	73	0.03
336 Lacadiera	May 2007	4 April 2010	3.39	12.71	0.03	8.34	14.4	2.04	2.19	68	0.12
1036 Ganymed	May 2007	14 Oct. 2010	4.45	11.30	0.46	7.05	15.0	2.98	3.95	11	0.74
8 Flora	Jan. 2009	24 Sept. 2011	3.36	13.56	0.00	8.14	14.8	2.19	2.95	33	0.09
21 Lutetia	Dec. 2008	14 Aug. 2012	4.19	10.44	0.50	13.49	14.5	2.36	2.68	61	0.03
40 Harmonia	Jan. 2009	29 April 2011	3.04	9.22	0.00	5.69	13.6	2.17	2.90	36	0.25
75 Eurydike	Dec. 2008	3 July 2011	3.19	10.20	0.00	10.67	14.1	2.16	2.86	38	0.08
80 Sappho	Jan. 2009	20 Aug. 2011	3.07	9.06	0.00	11.43	13.7	1.89	1.72	83	0.08
115 Thyra	Dec. 2008	24 March 2011	3.06	14.45	0.13	5.55	13.5	2.20	3.07	24	0.64
406 Erna	Feb. 2009	24 Dec. 2011	4.33	14.46	0.00	4.81	15.3	3.22	2.47	132	0.33
613 Ginevra	Dec. 2008	2 March 2011	4.20	11.00	0.37	8.99	14.5	2.83	3.80	10	0.90
7 Iris	Aug. 2010	12 Nov. 2012	4.30	12.31	0.00	9.85	14.6	2.80	3.70	21	0.96
27 Euterpe	July 2010	3 Jan. 2014	4.19	10.75	0.50	8.34	14.3	2.74	3.66	17	0.04
33 Polyhymnia	Aug. 2010	6 June 2014	4.21	15.00	0.22	9.55	14.4	2.02	1.59	99	0.10
44 Nysa	Sept. 2010	18 Dec. 2012	4.32	13.00	0.00	8.63	15.3	2.77	3.57	30	0.94
55 Pandora	Aug. 2010	26 May 2014	4.30	11.59	0.00	10.07	14.8	2.41	2.75	60	0.10
140 Siwa	Sept. 2010	22 June 2014	4.30	11.51	0.00	14.42	14.9	2.28	2.38	72	0.04
161 Athor	Sept. 2010	7 June 2013	3.31	12.12	0.00	9.47	15.1	2.16	2.66	50	0.13
336 Lacadiera	Sept. 2010	16 July 2014	4.32	12.97	0.04	12.54	15.3	2.33	2.54	67	0.03

extended mission and that only require orbit corrections maneuvers, as well as a maneuver to avoid atmospheric reentry.

A few mission options including secondary targets and extensions are considered next. Tables 3–5 give the following mission parameters: names of the celestial bodies; diameters and taxonomic types of the encountered asteroids; date of launch and dates of the bodies flyby; outgoing excess velocity for the launch, incoming excess velocities for the gravity assists, and flyby velocities for the encountered asteroids; minimal altitudes of the initial low Earth orbit and planets swingbys; distances in astronomical units (AU) from the sun and Earth during the asteroid encounter; S–E–SC angle during the encounter; and illumination phase of the celestial bodies as seen from the approaching spacecraft (from the departing spacecraft for the launch). The close approach to the secondary targets needs the additional ΔV given in the footnotes. Tables 3–5 do not give the spacecraft withdrawal ΔV necessary for the extended missions because they depend on the capsule reentry angle and the capsule separation time.

16 Psyche Primary Target (Launch in 2004)

The 16 Psyche sample-return mission can include three secondary targets, using an additional ΔV of 300 m/s: the very large asteroid

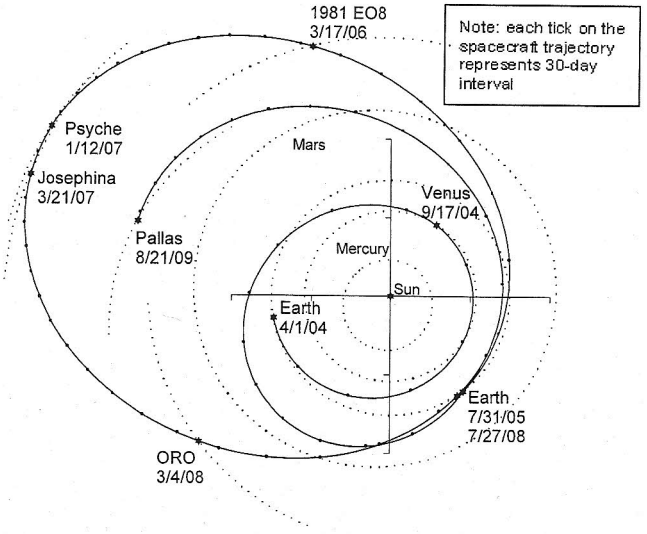

Fig. 2 Spacecraft trajectory for the Psyche sample-return mission.

Table 3 Psyche sample return mission including secondary targets and extensions[a]

Name	Diameter, km	Taxonomy type	Date of flyby	Hyperbolic approach velocity, km/s	Periapsis height, km	Distance from sun, AU	Distance from Earth, AU	S–E–SC angle, deg	Phase (1 = full)
Earth			1 April 2004	2.95	200	1.00	0.00	0	0.53
Venus			17 Sept. 2004	5.60	11,600	0.72	0.94	43	0.89
Earth			31 July 2005	9.24	300	1.02	0.00	0	0.00
8457 1981 EO8	6.8[a]		17 March 2001	10.44		2.23	2.08	85	0.93
16 Psyche	264.0	M	12 Jan. 2007	4.58		3.18	2.55	122	0.43
303 Josephina	103.0		21 March 2007	5.71		3.19	2.26	154	0.34
4733 ORO	6.2[b]		4 March 2008	12.55		2.03	1.66	97	0.03
Earth			27 July 2008	9.63	2,700	1.02	0.00	0	0.12
2 Pallas	525.0	B	21 Aug. 2009	14.60		2.57	2.74	70	0.83
			or						
Earth			27 July 2008	9.61	8,400	1.02	0.00	0	0.12
4 Vesta	510.0	V	21 Aug. 2010	8.45		2.45	2.29	87	0.88

[a]Launch $C_3 = 8.71$ km^2/s^2, midcourse $\Delta V = 0.30$ km/s.
[b]Diameter calculated assuming albedo = 0.15.

Table 4 Angelina or Aschera sample return mission including extensions[a]

Name	Diameter, km	Taxonomy type	Date of flyby	Hyperbolic approach velocity, km/s	Periapsis height, km	Distance from sun, AU	Distance from Earth, AU	S–E–SC angle, deg	Phase (1 = full)
Earth			3 Nov. 2005	3.18	200	0.99	0.00	0	0.57
Venus			1 April 2006	5.27	12,800	0.72	0.74	46	0.72
Earth			7 Feb. 2007	9.35	300	0.99	0.00	0	0.00
64 Angelina	63.1[b]	E	15 March 2008	6.96		2.99	3.91	19	0.90
214 Aschera	26.8	E	4 June 2009	8.78		2.61	3.38	34	0.08
Earth			9 Feb. 2010	9.49	1,500	0.99	0.00	0	0.13
12 Victoria	117.0	S	25 June 2010	20.66		2.33	2.07	92	0.91
			or						
Earth			9 Feb. 2010	9.53	17,200	0.99	0.00	0	0.13
27 Euterpe	131.0	S	19 Oct. 2010	13.29		2.65	2.93	64	0.89

[a]Launch $C_3 = 10.11$ km^2/s^2, midcourse $\Delta V = 0.37$ km/s.
[b]Diameter was calculated assuming albedo = 0.38 typical for the E-type asteroids.

Table 5 Nysa or Lacadiera sample return mission including extensions[a]

Name	Diameter, km	Taxonomy type	Date of flyby	Hyperbolic approach velocity, km/s	Periapsis height, km	Distance from sun, AU	Distance from Earth, AU	S–E–SC angle, deg	Phase (1 = full)
Earth			27 Sept. 2010	3.56	200	1.00	0.00	0	0.52
Venus			12 March 2011	7.59	10,300	0.73	1.13	39	0.97
Earth			20 Jan. 2012	10.63	400	0.98	0.00	0	0.00
44 Nysa	73.3	E	16 Dec. 2012	8.74		2.77	3.56	31	0.94
336 Lacadiera	72.0	D	16 July 2014	12.56		2.33	2.54	67	0.03
Earth			20 Jan. 2015	10.62	14,300	0.98	0.00	0	0.09
2 Pallas	525.0	B	6 Jan. 2017	9.71		2.89	3.33	55	0.83
			or						
Earth			20 Jan. 2015	10.57	4,500	0.98	0.00	0	0.09
135 Hertha	82.0	M	14 Sept. 2015	10.44		2.34	2.86	49	0.86

[a]Launch $C_3 = 12.65$ km^2/s^2, midcourse $\Delta V = 0.21$ km/s.

303 Josephina, 2 Pallas, and 4 Vesta. Table 3 gives the mission parameters and also shows that the flight to Vesta takes more than two years after the main mission. The Earth flyby altitude also is higher in the case of Vesta, which leads to the higher spacecraft withdrawal ΔV. Figure 2 shows the mission for Pallas as an extended target. Note that if Vesta is the extended target, then one more asteroid 4667 Robbiesh can be approached before the Vesta encounter (on 15 January 2010) for an additional ΔV of about 90 m/s.

64 Angelina or 214 Aschera Primary Target (Launch in 2005)

Table 4 shows another mission option to be launched in 2005. As is seen in Table 4, the two E-type 64 Angelina and 214 Aschera primary targets can be reached in one mission. One of them has to be treated as a secondary target because both of the asteroids are of the same taxonomic type. Otherwise Aschera can be considered as a backup primary target if the Angelina sample collection fails. This particular selection raises the mission reliability, although two projectiles are needed. As is seen in Table 4, 12 Victoria and 27 Euterpe asteroids are among the possible extended mission targets. The Victoria extended mission is very short, just 4.5 months, and the encounter conditions are better for this option than in case of the Euterpe extended mission (distances from the sun and Earth are shorter). The Earth flyby altitude and the necessary spacecraft withdrawal ΔV, respectively, are quite low for the Victoria extended mission. However, as is seen in Table 4, Victoria flyby velocity is quite high, 20.7 km/s.

44 Nysa and 336 Lacadiera Primary Targets (Launch in 2010)

Table 5 shows that the missions to the 64 Angelina and 214 Aschera asteroids to be launched in 2010 can be combined in one mission. The asteroids are of different taxonomic types; therefore, it would be interesting to take samples from both of them. There are no other secondary targets for the mission with an acceptable additional ΔV. As is seen in Table 5, 2 Pallas and 135 Hertha are among the possible extended mission targets. Hertha is a convenient secondary target because the extended mission duration to it is rather short, about eight months (most of the other interesting extended mission options have their duration longer than one year). The Earth flyby

altitude and the spacecraft withdrawal ΔV, respectively, are also much smaller for Hertha than for Pallas.

Spacecraft Navigation

The spacecraft motion relative to the encountered asteroid is approximately uniform and rectilinear, in the vicinity of the closest approach. For instance, the difference in the spacecraft relative velocity near the closest approach, as well as in the previous 10 days, does not exceed 40 m/s and 0.15 deg in the velocity value and direction, respectively, for any mission option. Therefore, we can assume that the spacecraft relative velocity is constant in the vicinity of the closest approach; this assumption simplifies the subsequent analysis.

To fulfill the mission goal, the spacecraft has to approach the asteroid very closely. This very close approach is possible only using an autonomous optical navigation. All of the primary targets considered are bright, and the onboard observations of the asteroids can begin quite long before the closest approach if sensitivity of the spacecraft camera is higher than 8 stellar magnitude. Even the relatively small 317 Roxane asteroid with poor approach conditions (phase = 0.04; see Table 2) is bright enough to be observed from the spacecraft quite in advance.

DS1 has proven[3] that the autonomous navigation can lower the uncertainty of the relative spacecraft-to-asteroid position down to 3 km in B-plane and allow the spacecraft to approach the asteroid to the distance of 15 km. However, it may be necessary to provide smaller relative position uncertainty and closer approach to the asteroid for the sample-return mission. The autonomous navigation system similar to DS1 can provide the crosstrack error in the mutual spacecraft and asteroid position down to 0.5 km in 6 h before the closest approach.[8] However, this error holds true only for a small asteroid because of the asteroid centroiding problem. The problem appears due to the not full illumination phase of the asteroids as is seen from the approaching spacecraft and the possible irregular asteroid shape. Assuming that the asteroid can be centroided with an error of 1% of its diameter (which is quite optimistic), we obtain the error of about 5 km for Pallas and Vesta, about 2 km for Psyche, and more than 1 km for several other mission options (see Table 1). There is another serious problem of the spacecraft and projectile targeting: The asteroid of an uncertain, irregular shape can put its elongated part in the spacecraft path during the closest approach, which will lead to the spacecraft collision with the asteroid. Or, vice versa, the asteroid can turn by its short side at the projectile approach time, and the projectile will miss the asteroid. There are various possible solutions of the problem. For instance, the simplest solution is to consider only small asteroids for the sample-return mission, for example, of 5–10 km in diameter. One possible solution is to use (for the navigation only) the asteroid images obtained exactly at times equal to integer numbers of the asteroid rotation period. In this case, the asteroid will be in the same attitude at the closest approach as it will have been seen in the images used for the spacecraft and projectile targeting. The asteroid centroiding also is not needed in this case: The spacecraft motion can be determined with respect to the asteroid illuminated limb. The rotation periods are known for most of the asteroids considered as the primary mission targets[6,9] (see Table 1). The following assumptions are used: 1) the onboard observations of the asteroid begin 10 days and end one asteroid rotation period before the closest approach, 2) the reference star positions in the onboard catalog are accurate to 1 arc-s (5 μrad), and 3) angular resolution of the spacecraft camera is 2 arc-s [10 μrad; the DS1 MICAS camera resolution was 13 μrad (Ref. 10), although the initial requirement was 5 μrad (Ref. 8)]. Therefore, the asteroid and star positions in the camera image can be measured with errors within 1 arc-s. Assuming that the errors in the same image are independent, and taking into account the independent errors of the reference star catalog, one can obtain the asteroid angular position with accuracy of about $\sqrt{(3)} \approx 1.7$ arc-s (8.4 μrad). The final assumption is that the errors of different observations separated by one or more asteroid rotation periods are independent.

The proposed navigation method gives an error in the B-plane within 1.5 km one asteroid rotation period before the closest approach for the following considered primary targets: 4 Vesta (error 0.8 km), 16 Psyche (0.5 km), 40 Harmonia (1.5 km), 55 Pandora (0.8 km), 115 Thyra (1.2 km), 250 Bettina (1.0 km), 317 Roxane (1.4 km). For all other asteroids with known rotation periods, the errors are between 1.6 and 8 km. Thus, this simple and elegant solution provides quite good accuracy of the spacecraft-to-asteroid position in the B-plane for a few mission options.

Note that the time of the closest approach carries an error, which, nevertheless, will not significantly influence the suggested method. The procedure assumes an uncertainty in the relative spacecraft and asteroid position equal to 300 km along the spacecraft path. Then, as can be easily calculated from the asteroid rotation period and the spacecraft flyby velocity, the error in the asteroid attitude will be of about 1.5 deg for Psyche and less than 1 deg for other asteroids. This error cannot noticeably change the asteroid cross section orthogonal to the spacecraft path.

The rotation periods of some of the asteroids contains rather large errors.[6,9] However, the knowledge of the rotation periods can be improved before the mission using more asteroid observations.

A more technically complex solution yet is to consider a maneuvering projectile. The projectile can be controlled by the main spacecraft (the case of a spin-stabilized projectile propelled by a pressurized cold gas is shown in Fig. 3). The projectile can be designed as a small autonomous spacecraft targeting itself to the asteroid. In all cases, a secondary target encountered before the primary one can be used for the navigation testing.

Projectile Targeting

Figure 4 illustrates the projectile targeting. When it is assumed that $t_s > 0$, $\tau > 0$, and $t_s \gg \tau$, the ejected particles will have widely varying velocities after the impact. However, considering a typical ejection velocity u provides $\tau \approx h/u$. The necessary condition for the ejection of a considerable amount of the sample using the impact energy is

$$u \ll v \tag{1}$$

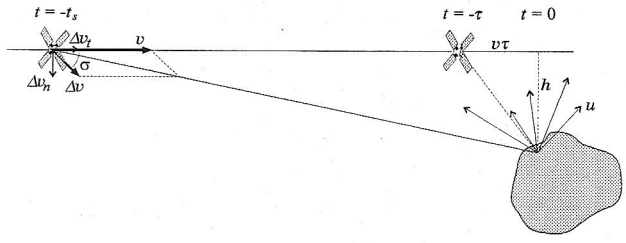

Fig. 4 Projectile targeting.

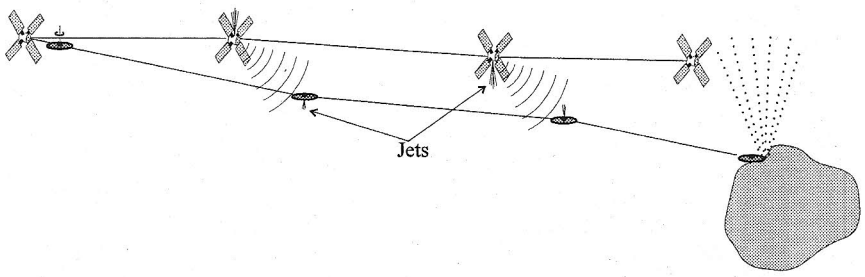

Fig. 3 Active spacecraft and projectile targeting till the impact.

The sample ejection velocities and the delay time τ are considered in more detail in the next section of the paper. In the framework of the considered uniform linear motion model

$$\Delta v_n = h/t_s, \qquad \Delta v_t = v(\tau/t_s) \tag{2}$$

Then

$$\tan\sigma = \Delta v_n/\Delta v_t = h/v\tau \approx u/v \ll 1 \tag{3}$$

Thus, the separation angle is small and does not depend on the separation time and flyby distance and

$$\Delta v = \sqrt{\Delta v_t^2 + \Delta v_n^2} \approx \Delta v_t \tag{4}$$

Consider the projectile angular separation error $\delta\sigma$. The uncertainty in the distance h stipulated by the error is

$$\delta h = \Delta v_n t_s \delta\sigma = v\tau\delta\sigma \approx (v/u)\, h\delta\sigma \tag{5}$$

Thus, the uncertainty also does not depend on the separation time and flyby distance. Because the uncertainty and the projectile separation error are independent, the projectile miss D of the nominal impact point in the B-plane is

$$D = \sqrt{\delta d^2 + \delta h^2} \tag{6}$$

The miss distance is very important for the projectile targeting because it determines the maximum limit for the distance of the targeting point to the asteroid local horizon. Error in the separation velocity value only influences the delay time τ and is not as important.

Sample Ejection

Inert Projectile

In this case a projectile produces the asteroid sample ejection by means of the impact energy. Because the impact velocity is nearly equal to the spacecraft flyby velocity v, then the impact energy is

$$E = mv^2/2 \tag{7}$$

where m is the projectile mass. Speeifie impact energy is quite high for the mission options considered here and varies from 8.4 to 103 MJ/1 kg of the projectile mass (see flyby velocities in Table 2). However, only part ηE of the energy can be transformed into the ejection, where η is the impact effectiveness. The effectiveness is low because a significant part of the impact energy is transformed into heating. It may be reasonable to drop a cluster of projectiles (as it is proposed for the Aladdin mission[2]) covering an area under the spacecraft path. This cluster of projectiles can raise the mission reliability because a single projectile hitting a rock can produce an aside ejection that does not cross the spacecraft flyby trajectory. Several projectiles separated with slightly different separation angles can compensate the uncertainty in Eq. (5) due to the separation error.

Exploding Projectile

Considering a projectile containing an explosive inside, the explosion energy is

$$E = \chi m_e \tag{8}$$

The highest values for χ (1.4 MJ/kg) are found for the explosives hexogen (RDX) and octogen (HMX).[11] This energy is much lower than the projectile impact energy. However, using explosive has a few advantages, such as the following. First, a pencil-like-shaped projectile can penetrate the asteroid to some depth, and then the explosion will provide samples from deeper layers. Second, the effectiveness η of the explosion probably can be higher than the one with the impact. Third, perhaps it is possible to direct the explosion upward somehow, thus raising the spatial density of the dust cloud in the way of the spacecraft. It is also possible to increase the transferred energy by using both the impact energy and the explosion for the ejection.

Ejection Model

Assuming that the asteroid particles are ejected with velocities u uniformly distributed between 0 and U, that is, the ejected mass having velocity u is

$$\mathrm{d}M(u) = \lambda\, \mathrm{d}u$$

where λ is a constant. Because the entire ejected mass is

$$M = \int_0^M \mathrm{d}M = \lambda \int_0^U \mathrm{d}u = \lambda U$$

it follows that

$$\mathrm{d}M(u) = \frac{M}{U}\,\mathrm{d}u \tag{9}$$

The effective energy transformed into the ejection of the mass M is

$$\eta E = \frac{1}{2}\int_0^M u^2\,\mathrm{d}M = \frac{M}{2U}\int_0^U u^2\,\mathrm{d}u = \frac{MU^2}{6}$$

Thus,

$$M = 6\eta E/U^2 \tag{10}$$

The model assumes that the projectile impact or explosion energy, transformed into the sample ejection, dissipates uniformly between two circular conical sectors with axis collinear to the projectile velocity and apex angles φ_1 and φ_2, respectively, and sector angle ψ (Fig. 5). This model is quite general because by varying the angles it provides different shapes of the ejected cloud. Gravitational acceleration near the considered asteroids (see Table 1) is within 0.25 m/s^2. Therefore, it is possible to neglect the ejection velocity change during a few tens of seconds if the velocity is in the order of 100 m/s. Then, the volume of the dust cloud in time τ after the impact will be $= \psi c R^3/3$, where $R = U\tau$ is the maximum particle distance from the impact, $c = \cos\varphi_1 - \cos\varphi_2$. Elementary volume at the distance $r = u\tau \le R$ from the impact is

$$\mathrm{d}V(r) = \psi c r^2\,\mathrm{d}r$$

Equation (9) gives

$$\mathrm{d}M(r) = \frac{M}{R}\,\mathrm{d}r$$

The spatial density of the dust cloud at the distance r from the impact, using Eq. (10), can be found as

$$\rho(r) = \frac{\mathrm{d}M}{\mathrm{d}V} = \frac{M}{\psi c r^2 R} = \frac{6\eta E}{\psi c r^2 R U^2} \tag{11}$$

Sample Collection

Because of condition (1), it is assumed that the ejected dust cloud is not changed during the time of its crossing by the spacecraft. The mass μ of the collected sample can be estimated as follows:

$$\mu = S\int_{x_1}^{x_0} \rho(r)\,\mathrm{d}x$$

where S is area of the sample collector, x is the spacecraft position in the flyby trajectory counted from the closest approach to the impact,

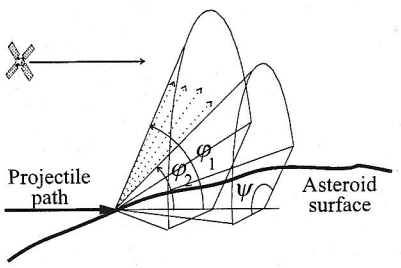

Fig. 5 Sample ejection model.

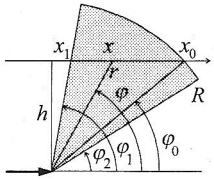

Fig. 6 Crossing the dust cloud.

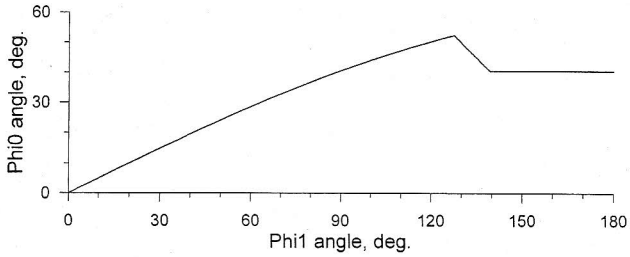

Fig. 7 Optimal φ_0 angle vs φ_1 angle.

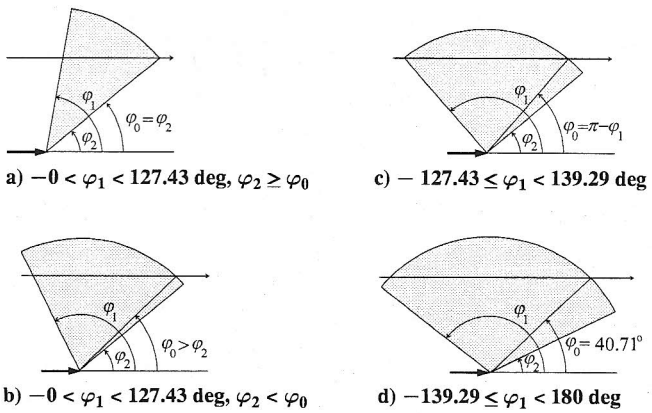

a) $-0 < \varphi_1 < 127.43$ deg, $\varphi_2 \geq \varphi_0$ **c) $-127.43 \leq \varphi_1 < 139.29$ deg**

b) $-0 < \varphi_1 < 127.43$ deg, $\varphi_2 < \varphi_0$ **d) $-139.29 \leq \varphi_1 < 180$ deg**

Fig. 8 Different cases of the optimal crossing of the dust cloud.

$x = h \cot\varphi$ (Fig. 6). Taking into account Eq. (11) and relations $r = h/\sin\varphi$ and $R = h/\sin\varphi_0$, then

$$\mu = \frac{6\eta ES}{\psi chRU^2}\int_{\varphi_0}^{\varphi_1} d\varphi = \frac{6\eta ES}{\psi ch^2U^2}(\varphi_1 - \varphi_0)\sin\varphi_0 \qquad (12)$$

Note that in a particular case angle φ_0 can be equal to φ_2. It is assumed that the parameters U, φ_1, and φ_2 are a priori known; they can be estimated theoretically or by means of ground experiments if there is a guess about the asteroid soil hardness and cohesion. It is assumed that

$$\varphi_2 \leq \varphi_1, \qquad \varphi_2 \leq \pi - \varphi_1 \qquad (13)$$

An optimal value of the angle φ_0 providing the maximum in Eq. (12) can be easily found. Note that the necessary condition of $\max_{\varphi_0}(\varphi_1 - \varphi_0)\sin\varphi_0$ is the equation

$$\varphi_0 + \tan\varphi_0 = \varphi_1 \qquad (14)$$

As is seen from Eq. (14), $\varphi_0 < \varphi_1/2$, the optimal value of φ_0 vs φ_1 angle is given in Fig. 7. There are four different cases shown in Fig. 8: 1) $0 < \varphi_1 < 127.43$ deg and $\varphi_2 \geq \varphi_0$, where φ_0 is defined by Fig. 7, then optimal $\varphi_0 = \varphi_2$ (Fig. 8a); 2) $0 < \varphi_1 < 127.43$ deg and $\varphi_2 < \varphi_0$, where φ_0 is defined by Fig. 7, then optimal φ_0 is given by the ascending curve in Fig. 7 (Fig. 8b); 3) $127.43 \leq \varphi_1 < 139.29$ deg, then optimal $\varphi_0 = 180$ deg $- \varphi_1$ (Fig. 8c); and 4) $139.29 \leq \varphi_1 < 180$ deg, then optimal $\varphi_0 = 40.71$ deg (Fig. 8d).

Note that the parameters E, η, ψ, and h do not influence the optimal flyby configuration. Note that the second constraint of Eq. (13) is empirical and means that the ejection resultant cannot be directed backward with respect to the projectile motion. However all results given earlier can be easily generalized for the case $\varphi_2 > \pi - \varphi_1$. After the φ_0 angle value is found, the delay time τ can be calculated as follows:

$$\tau = R/U = h/U\sin\varphi_0 \qquad (15)$$

Consider the particular case when $90 < \varphi_1 \leq 139.29$ deg, $\varphi_2 = 180$ deg $- \varphi_1$, and $\psi = 180$ deg, which corresponds, for example, to an explosion in all directions orthogonal to the projectile longitudinal axis ejecting the asteroid soil in upper hemisphere. In this case $\varphi_0 = \varphi_2$ and Eq. (12) gives

$$\mu = (3\eta ES/\pi h^2U^2)(\pi - 2\varphi_2)\tan\varphi_2 \qquad (16)$$

Note that the Eqs. (12) and (16) are very approximate because of inevitable uncertainties in the h, η, U, φ_1, φ_2, and ψ parameters and the assumption about the uniform distribution of the ejection velocities. Neither of these expressions can be used directly for the spacecraft targeting. For instance, due to a possible error in h value, it is reasonable to increase a little the delay time τ to not miss the dust cloud. This delay time increase will lead to a lower spatial density of the crossed dust cloud and higher projectile separation velocity in the value $\Delta\tau/\tau$, where $\Delta\tau$ is the delay time increment. Nevertheless, the results obtained allow one estimation of the collectable sample amount; in addition, the delay time τ and projectile separation velocity Δv can be estimated from Eqs. (2), (4), and (15).

Numerical Example

Considering the 16 Psyche sample return mission to be launched in 2004 (see Table 2 and Fig. 2). This option is quite good because the asteroid itself is of a certain interest, the launch C_3 and flyby velocity are very low compared with other options, and there are three possible secondary targets. However, the launch date for this option is too close in the future.

The example assumes that the onboard observations of the asteroid begin 10 days before the closest approach (CA). At that time the spacecraft will be at 3.9×10^6 km from Psyche, the asteroid angular diameter will be about 14 arc-s (67 μrad), and its brightness will be of 1.5 magnitude. Considering the autonomous navigation method, which uses only images made in time multiples of the asteroid rotation period (which equals 4.196 h for Psyche[6,9,12]; see Table 1). The example also assumes that the maximum observation error in inertial space is 1.73 arc-s (8.4 μrad) and that the uncertainties in the spacecraft position and velocity with respect to the asteroid due to the ground observations are 300 km and 1 m/s, respectively. Figure 9 gives the maximum error of the flyby altitude determination by means of the onboard observations vs observation time. Two days before CA (after the 46th observation, when the error is 5 km, see Fig. 9) the example supposes that the first trajectory correction maneuver (TCM1) is performed, targeting the spacecraft in about 10 km above the asteroid limb. The flyby altitude uncertainty defines

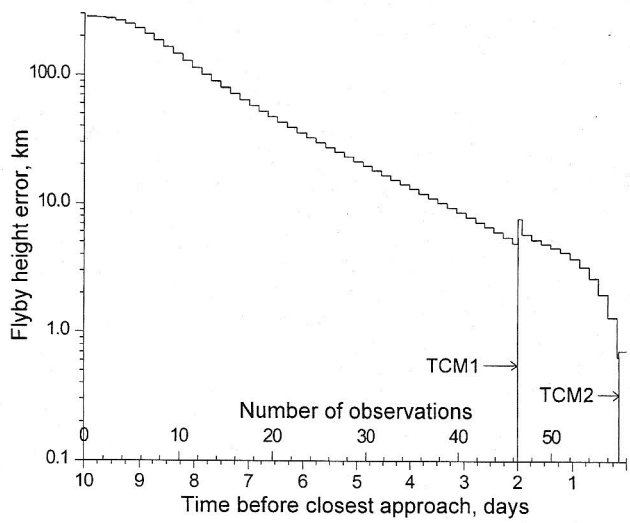

Fig. 9 Error of the flyby altitude determination for 16 Psyche asteroid.

the error to be corrected by the maneuver, due to the ground observations, assuming that the error is maximum, that is, equal to 300 km. In this case the TCM1 value is about 1.7 m/s. As is seen in Fig. 9, the maneuver deteriorates the altitude determination accuracy due to an error in the maneuver execution. The calculation assumes that the error is random and equal to 2% of the maneuver value in any direction. The last, 57th, onboard observation is made 4.196 h before CA. About 40 min after this observation (3.5 h before CA), the second trajectory correction maneuver (TCM2) is carried out targeting the spacecraft 3 km above the asteroid limb. Assuming that TCM2 corrects 15-km offset in B-plane (7-km difference between the first and second targeting plus 7.8-km error after TCM1; see Fig. 9), then TCM2 is about 1.2 m/s. The final flyby altitude error, taking into account TCM2 execution error, is about 0.7 km (see Fig. 9). This error is larger than the error mentioned in the discussion of spacecraft navigation (0.5 km) because errors of the correction maneuver executions were not taken into account in that section. However, note that the example considers the worst cases, when both TCM1 and TCM2 have maximum values. The 2% execution value is also rather pessimistic. Therefore, it can be expected that the real Psyche flyby altitude uncertainty will be between 0.5 and 0.7 km.

The example is for a projectile separation 30 min after TCM2, that is, 3 h before CA, targeted 2 km below the asteroid local horizon. Thus, the nominal value of the h distance is 5 km. A sample collector area of 0.5 m^2 is assumed, which is much bigger than the 0.1-m^2 Stardust spacecraft collector.[1]

When it is assumed that several 1-kg inert projectiles separated from the spacecraft and that a successful impact produces an ejection with efficiency $\eta = 0.1$, ejection angles $\varphi_1 = 90$ deg, $\varphi_2 = 45$ deg, and $\psi = 120$ deg (see Fig. 5), and a maximum ejection velocity $U = 200$ m/s, then the values of the parameters of the projectiles separation, impact, and the sample collection are the following: $\Delta v = 14.8$ m/s, $\sigma = 1.8$ deg, $\delta h = 0.9$ km, $D = 1.2$ km, $\tau = 35$ s, $\varphi_0 = 45$ deg, and $\mu = 1.2$ mg for each successful impact. When it is assumed that the projectile mass is 10 kg, the explosive mass is 5 kg, the explosion efficiency $\eta = 0.3$, the maximum ejection velocity is $U = 500$ m/s, the ejection angles are $\varphi_1 = 120$ deg, $\varphi_2 = 60$ deg, and $\psi = 120$ deg. Then $\Delta v = 4.9$ m/s, $\sigma = 5.5$ deg, $\delta h = 0.3$ km, $D = 0.8$ km, $\tau = 12$ s, $\varphi_0 = 60$ deg, and $\mu = 0.2$ mg.

Thus, for the considered example, the maximum collected mass can be on the order of 0.1–1 mg. Note that the goal of the Stardust mission is to recover more than 1000 comet dust particles larger than 15 μm diameter; the mass of this amount is of order of 0.01 mg.

Note that the demands to the projectile targeting accuracy can be lowered if the projectile separation time is closer to the impact time. The short time between these two events also will give more time for the orbit determination and projectile targeting. However, in this case the projectile separation velocity will increase. As is seen in the numerical example, this increment is quite possible for the case of the projectile explosion with the considered parameters, for which the separation velocity is low. Note that if the projectile separation mechanism is available, it may be reasonable to calculate the separation time assuming the separation velocity as large as the mechanism permits.

Conclusions

The paper proposes a flyby main-belt asteroid sample-return mission, that is, one without landing on the asteroid. The sample is collected when the spacecraft crosses the dust cloud produced by a projectile that is detached from the spacecraft. The sample is then returned to the Earth. The mission uses VEGA maneuvers, which considerably lower the required launch ΔV. The VEGA maneuver and the absence of substantial midcourse active maneuvers significantly lowers the spacecraft total mass, launcher requirements, and, hence, mission costs.

We consider five launch windows within the 2004–2010 period as examples, with many different asteroid mission options and their respective trajectory design. Most missions can be extended to encounter secondary asteroid targets. Possible navigation alternatives for the asteroid flybys are presented. Projectile targeting, asteroid dust ejection, and the sample collection are modeled and numerical simulation results are presented. The presented results indicate the feasibility of a main-belt sample-return mission with relatively low cost.

Further studies, however, are needed to deal with potential difficulties in the proposed sample-return missions. For example, the engineering of the projectile subsystem or the uncertainties about the properties of the asteroid surface must be investigated. Our analysis assumes the use of known solutions for the sample collector and the recoverable capsule, such as those designed for the Stardust aerogel panel and the Aladdin conical concentrators, respectively. Nevertheless, other solutions to the sample collector design may be recommended after further study.

Acknowledgments

The authors are grateful to L. O. Ferreira and D. B. Netto, from the National Space Research Institute, for extremely useful discussions and invaluable information about properties of explosions and hypervelocity impacts. Also acknowledgements go to J. E. Riedel, from the Jet Propulsion Laboratory, for valuable electronic discussions about imaging navigation for the spacecraft.

References

[1]Eismont, N. A., and Sukhanov, A. A., "Low Cost Phobos Sample Return Mission," *Proceedings of the 12th Symposium On Space Flight Dynamics*, ESA/ESOC, 1997, pp. 365–370.

[2]Watson, J. G., "NASA's Deep Space 1 Succeeds in Close Asteroid Flyby" [online], URL: http://neo.jpl.nasa.gov/news/news051.html [cited 29 July 1999].

[3]Dornheim, M. A., "DS1 Asteroid Flyby Yields Uncertain Results," *Aviation Week and Space Technology*, 2 Aug. 1999, p. 32.

[4]Gaffey, M. J., Burbine, T. H., and Binzel, R. P., "Asteroid Spectroscopy: Progress and Perspectives," *Meteoritics*, Vol. 18, June 1993, pp. 161–187.

[5]Tholen, D. J., and Barucci, M. A., "Asteroid Taxonomy," *Asteroids II*, edited by R. P. Binzel, T. Geherels, and M. S. Matthews, Univ. of Arizona Press, Tucson, AZ, 1989, pp. 298–315.

[6]Lagerkvist, C.-I., "Rotation Periods of Asteroids. Version VIII" [online], URL: http://www.astro.uu.se/planet/ rotast_eng.html [cited 28 Aug. 1996].

[7]Bowell, E., "The Asteroid Orbital Elements Database" [online], URL: ftp://ftp.lowell.edu/pub/elgb/astorb.html [cited April 1999].

[8]Riedel, J. E., Bhaskaran, S., Synnott, S. P., Desai, S. D., Bollman, W. E., Dumont, P. J., Halsell, C. A., Han, D., Kennedy, B. M., Null, G. W., Owen, W. M., Jr., Werner, R. A., and Williams, B. G., "Navigation for the New Millennium: Autonomous Navigation for Deep Space 1," *Proceedings of the 12th International Symposium on Space Flight Dynamics*, ESA/ESOC, 1997, pp. 303–320.

[9]Magnusson, P., "Files in SBN Data Set EAR-A-5-DDR-ASTEROID-SPIN-VECTORS-V4.0 (SPIN)" [online], URL: http://pdssbn.astro.umd.edu/SBNast/holdings/EAR-A-5-DDR-ASTEROID-SPIN-VECTORS-V4.0.html [cited 29 Dec. 1995].

[10]Rayman, M. D., Varghese, P., Lehman, D. H., and Livesay, L. L., "Results from the Deep Space 1 Technology Validation Mission," 50th International Astronautical Congress, International Academy of Astronautics, Paper IAA-99-IAA.11.2.01, Oct. 1999.

[11]Meyer, R., *Explosives*, 3rd ed., VCH Verlagsgesellschaft, Germany, 1987, p. 71.

[12]Zhou, X.-H., and Yang, X.-Y., "The Rotation of Asteroid (16) Psyche," *Chinese Astronomy and Astrophysics*, No. 6, 1982, pp. 57–59.

C. A. Kluever
Associate Editor